DOI: 10.1002/ejic.200900872

Pillared Layered Metal Phosphonates Showing Field-Induced Magnetic Transitions

Peng-Fei Wang,[a] Song-Song Bao,[a] Si-Min Zhang,[a] Deng-Ke Cao,[a] Xun-Gao Liu,[a] and Li-Min Zheng*[a]

Keywords: Copper / Cobalt / Phosphonates / Layered compounds / Metamagnetism / Spin flop

The first examples of metal phosphonates based on 6-phosphononicotinic acid ($pnaH_3$), namely, $M_3(pna)_2(H_2O)_2$ {**1**: M = Cu^{II}, **2**: M = Co^{II}} are reported. Both possess pillared layered structures. Within the inorganic layer, chains made up of dimers of edge-sharing $\{M2O_6\}$ octahedra and $\{M1O_6\}$ octahedra through O(1W), O–P–O, and O–C–O units are interconnected by $\{PO_3C\}$ tetrahedra. The pyridyl groups of pna^{3-} serve as the pillars. An antiferromagnetic ground state is found for each compound. When the external field reaches critical points at low temperature, compound **1** features a spin flop transition, whereas **2** shows metamagnetic behavior.

Introduction

Metal phosphonate chemistry has received increasing attention in recent years owing to potential applications in exchange and sorption,[1] catalysis,[2] optics,[3] magnetism,[4] and biotechnology.[5] Among the large number of metal phosphonate compounds reported thus far, many exhibit layered or pillared layered structures.[1a,6] Layered or pillared layered compounds with antiferromagnetic (AF) ground state are of interest, because they could provide good examples to understand some fundamental phenomena in magnetism such as spin canting, metamagnetic transition, spin flop transition, etc.[7–11] Despite the fact that most metal phosphonates with layered or pillared layered structures possess AF ground states, those displaying metamagnetism or spin flop behavior are rather limited in number, including $[NH_3(CH_2)_4NH_3][Cu_3(hedp)_2]\cdot 2H_2O$, $[NH_3(CH_2)_3NH_3][Cu_3(hedp)_2\cdot 3.5H_2O]$,[12] $Cu_4(hedp)_2(C_4H_4N_2)(H_2O)_4$,[13] $Na_6Co_7(hedp)_2(hedpH)_4(H_2O)_8\cdot H_2O$[14] {hedp = $CH_3C(OH)(PO_3)_2$}, $Co_3(O_3PCH_2NHC_5H_9COO)_2(O_3PCH_2NC_5H_{10})(H_2O)$,[15] $Co(2\text{-pmp})(H_2O)_2$ [2-pmp = $C_5H_4CH_2PO_3$],[16] and $Co_3(O_3PC_2H_4CO_2)_2$.[17]

In this paper, we present the first examples of metal phosphonates based on 6-phosphononicotinic acid ($pnaH_3$), namely, $M_3(pna)_2(H_2O)_2$ {**1**: M = Cu^{II}, **2**: M = Co^{II}}. Both show pillared layered structures; spin flop and metamagnetic transitions are observed for compounds **1** and **2**, respectively, at low temperature.

[a] State Key Laboratory of Coordination Chemistry, Coordination Chemistry Institute, School of Chemistry and Chemical Engineering, Nanjing University,
Nanjing 210093, P. R. China
Fax: +86-25-83314502
E-mail: lmzheng@nju.edu.cn

Supporting information for this article is available on the WWW under http://dx.doi.org/10.1002/ejic.200900872.

Results and Discussion

Description of Structures 1 and 2

Compound **1** crystallizes in the triclinic space group $P\bar{1}$, and its asymmetric building unit contains 1.5 Cu atom, one pna^{3-}, and one coordination water (Figure 1). The Cu1 atom sits in an inversion center, while Cu2 is in a general position. Both Cu1 and Cu2 are six-coordinate with a distorted octahedral coordination geometry. For Cu1, the equatorial positions are occupied by two phosphonate oxygen atoms (O3, O3C) and two carboxylate oxygen atoms (O4A, O4B) from four equivalent pna^{3-} ligands [Cu1–O 1.972(3)–1.932(3) Å]. Two equivalent water molecules (O1W and O1WC) fill in the axial positions [Cu1–O1W 2.560(3) Å]. For Cu2, four basal sites are occupied by a pyridine nitrogen (N1) and phosphonate oxygen atoms O1, O1D, and O2G from three equivalent pna^{3-} ligands with Cu2–O(N) distances of 1.929(3)–1.995(4) Å. The axial sites are provided by O1W and carboxylate O5H oxygen atoms [Cu2–O 2.426(3)–2.490(4) Å] (Table 1).

The pna^{3-} anion serves as a heptadentate ligand, chelating and bridging six Cu atoms through its one nitrogen and five oxygen donors (Scheme 1). The phosphonate oxygen O1 acts as a μ_3-O ligand and bridges two equivalent Cu atoms into a $\{Cu_2O_2\}$ dimer. The Cu2–O1–Cu2D bond angle and Cu2···Cu2D distance are 99.89(13)° and 3.048 Å, respectively. The dimers are connected by $\{Cu1O_6\}$ octahedra through O1W, O1–P1–O3, and O4–C6–O5 units, forming a chain running along the *b* axis. The neighboring chains are connected through O1–P1–O2 bridges, resulting in an undulating inorganic layer in the *ab* plane (Figure 2). The Cu1···Cu2 and Cu1···Cu2D distances are 4.305 Å and 4.590 Å, respectively. The inorganic layers are pillared by the pyridyl groups of the ligands, with an interlayer distance of 8.771 Å (Figure 3).

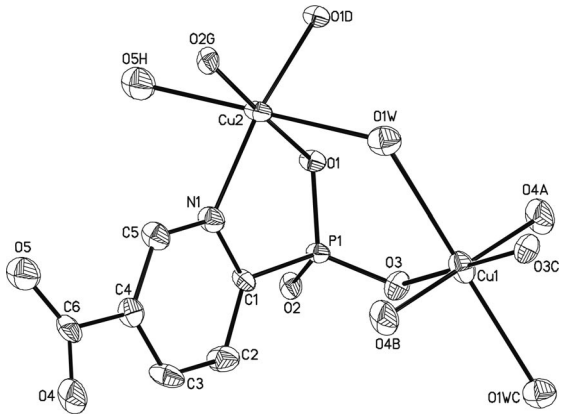

Figure 1. Building unit of **1** with atomic labeling scheme (50% probability). All H atoms are omitted for clarity.

Table 1. Selected bond lengths and angles for compound **1**.[a]

Bond lengths /Å			
Cu1–O4A	1.932(3)	Cu2–O2G	1.929(3)
Cu1–O3	1.972(3)	Cu2–O5H	2.490(4)
Cu1–O1W	2.560(3)	Cu2–O1W	2.426(3)
Cu2–N1	1.995(4)	P1–O1	1.537(3)
Cu2–O1	1.987(3)	P1–O2	1.494(3)
Cu2–O1D	1.994(3)	P1–O3	1.499(3)
Angles /°			
O4A–Cu1–O3	87.05(13)	O1–Cu2–O1D	80.11(13)
O3–Cu1–O1W	93.42(12)	O2G–Cu2–N1	95.53(14)
O4A–Cu1–O1W	97.57(13)	O1–Cu2–N1	86.11(14)
O2G–Cu2–O1	178.23(12)	O1D–Cu2–N1	166.22(14)
O2G–Cu2–O1D	98.23(12)	O2G–Cu2–O1W	96.31(12)
O1D–Cu2–O5H	92.34(12)	O1–Cu2–O1W	82.96(12)
O1W–Cu2–O5H	172.71(11)	O1D–Cu2–O1W	84.30(12)
O5H–Cu2–Cu2D	91.60(8)	N1–Cu2–O1W	94.82(14)
O2G–Cu2–O5H	90.56(13)	O1–Cu2–O5H	90.10(12)
N1–Cu2–O5H	86.89(14)	Cu2–O1–Cu2D	99.89(13)
Cu1–O1W–Cu2	119.38(13)		

[a] Symmetry transformations used to generate equivalent atoms: A, *x*, *y*, *z* – 1; B, –*x* + 1, –*y*, –*z* + 1; C, –*x* + 1, –*y*, –*z*; D, –*x* + 1, –*y* + 1, –*z*; E, *x* – 1, *y*, *z*; F, *x*, *y*, *z* + 1; G, *x* + 1, *y*, *z*; H, –*x* + 1, –*y* + 1, –*z* + 1.

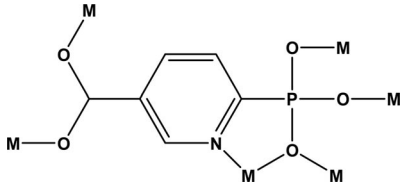

Scheme 1.

Compound **2** is isostructural to **1**. A pillared layered structure is again observed where the undulating inorganic layers are separated by organic groups (Figures 4 and 5). The Co1–O and Co2–O(N) distances are 2.040(3)–2.351(3) Å and 1.966(3)–2.281(3) Å, respectively (Table 2). The Co2···Co2D distance and Co2–O1–Co2D angle over the μ_3-O bridge are 3.148 Å and 97.93(1)°, respectively. The

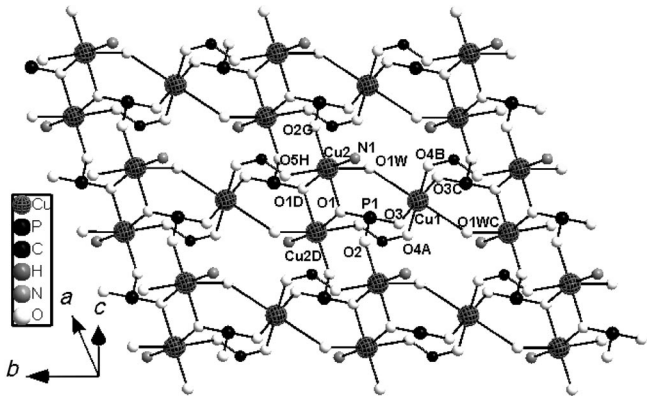

Figure 2. The inorganic layer in structure **1**.

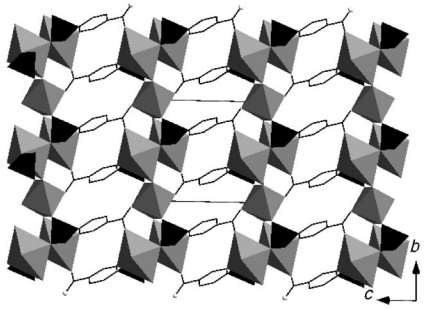

Figure 3. Pillared layered structure of **1** viewed along the *a* axis. $CuNO_5$ octahedra: gray, PO_3C tetrahedra: black.

Co1···Co2 and Co1···Co2D distances over the O1W, O1–P1–O3, and O4–C6–O5 bridges are 4.127 Å and 4.543 Å, respectively. The interlayer distance is 8.740 Å.

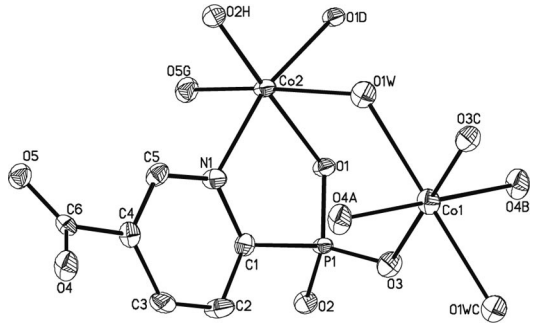

Figure 4. Building unit of **2** with atomic labeling scheme (50% probability). All H atoms are omitted for clarity.

It is worth mentioning that metal phosphonates incorporating pyridyl, carboxylate, and phosphonate groups in the same ligand are rarely described. A few examples include monomeric compounds, $[Cu(L)_2]\cdot 3H_2O$, $[Co(L)(H_2O)_3]\cdot H_2O$, and $[Ni(L)\cdot 0.5Ni(H_2O)_6]\cdot 2H_2O$ (H_3L = 6-phosphonopyridine-2-carboxylic acid),[18] a chain compound, $Cu(pinH_2)_2$, and a pillared layered compound, $Cu_3(pin)_2(H_2O)_2$ ($pinH_3$ = 2-phosphonoisonicotinic acid) (Scheme 2).[19] Compounds **1** and **2** provide the first examples of metal phosphonates based on 6-phosphononicotinic acid.

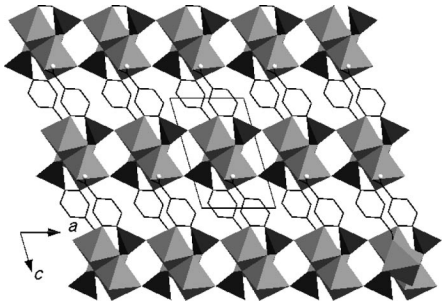

Figure 5. Pillared layered structure of **2** viewed along the *b* axis. $CoNO_5$ octahedra: gray, PO_3C tetrahedra: black.

Table 2. Selected bond lengths and angles for compound **2**.[a]

Bond lengths /Å			
Co1–O4A	2.040(3)	Co2–O1	2.112(3)
Co1–O3	2.069(3)	Co2–O5G	2.150(3)
Co1–O1W	2.351(3)	Co2–O1W	2.281(3)
Co2–O2H	1.966(3)	P1–O1	1.532(3)
Co2–O1D	2.061(3)	P1–O2	1.504(3)
Co2–N1	2.102(4)	P1–O3	1.518(3)
Angles /°			
O4A–Co1–O3	94.74(12)	O2H–Co2–O5G	97.24(12)
O4A–Co1–O1W	82.45(11)	O1–Co2–O5G	88.44(11)
O3–Co1–O1W	95.80(11)	N1–Co2–O5G	91.41(13)
O2H–Co2–O1	173.97(11)	O1D–Co2–O5G	90.78(11)
O2H–Co2–N1	93.88(12)	O2H–Co2–O1W	93.09(12)
O1–Co2–N1	83.91(12)	O1–Co2–O1W	81.41(11)
O2H–Co2–O1D	99.80(12)	N1–Co2–O1W	92.16(13)
O1–Co2–O1D	82.09(11)	O1D–Co2–O1W	83.22(11)
N1–Co2–O1D	165.76(12)	O5G–Co2–O1W	168.82(11)
Co1–O1W–Co2	125.98(14)	Co2–O1–Co2D	97.91(11)

[a] Symmetry transformations used to generate equivalent atoms: A, $-x + 1$, $-y+1$, $-z + 2$; B, x, y, $z - 1$; C, $-x + 1$, $-y + 1$, $-z + 1$; D, $-x + 1$, $-y + 2$, $-z + 1$; E, $x - 1$, y, z; F, x, y, $z + 1$; G, $-x + 1$, $-y + 2$, $-z + 2$; H, $x + 1$, y, z.

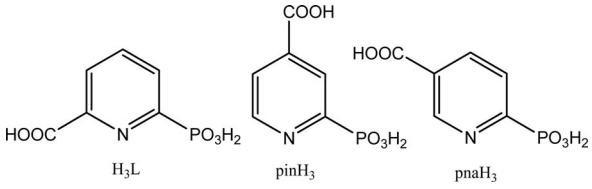

Scheme 2.

Interestingly, structure **1** is closely related to that of $Cu_3(pin)_2(H_2O)_2$,[19] although different phosphonate ligands are employed in the two cases. The main structural difference lies in three aspects: (1) the carboxylate group bridges two Cu^{II} ions in **1** ($Cu–O_{carboxy}$ 1.932, 2.490 Å), while it coordinates to one Cu^{II} ion in $Cu_3(pin)_2(H_2O)_2$ ($Cu–O_{carboxy}$ 1.952, 2.907 Å); (2) the Cu–O(P)–Cu angle in **1** (99.9°) is larger than that in $Cu_3(pin)_2(H_2O)_2$ (98.8°); (3) the interlayer distance in **1** (8.771 Å) is shorter than that in $Cu_3(pin)_2(H_2O)_2$ (9.021 Å). These structural differences are also reflected in the magnetic properties of the compounds.

Magnetic Properties of 1

The temperature-dependent molar magnetic susceptibilities of compound **1** were measured at 2 kOe in the temperature range 1.8–300 K. The observed $\chi_M T$ value per Cu_3 unit at 300 K is 1.37 $cm^3 K mol^{-1}$, which is close to the theoretical value (1.36 $cm^3 K mol^{-1}$) for three Cu^{II} ions with g = 2.2 (Figure 6). Above 9 K, the magnetic susceptibility obeys the Curie–Weiss law with a Curie constant of 1.36 $cm^3 K mol^{-1}$ and a Weiss constant of θ = +2.18 K. The positive θ value is indicative of a dominant ferromagnetic interaction between Cu^{II} centers, which is confirmed by the $\chi_M T$ vs. T curve. Upon cooling from room temperature, the $\chi_M T$ value increases continuously and reaches a maximum of 1.65 $cm^3 K mol^{-1}$ at 9.0 K, below which the $\chi_M T$ declines sharply to 0.36 $cm^3 K mol^{-1}$ at 2.0 K.

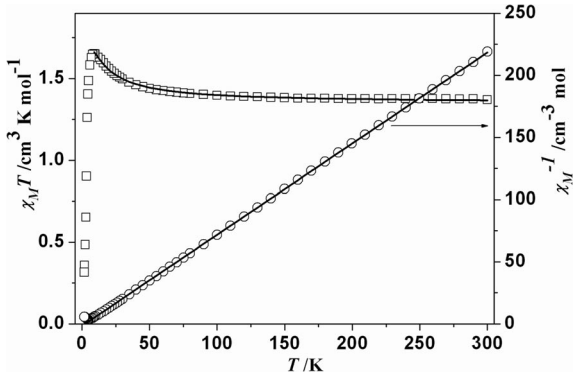

Figure 6. $\chi_M T$ and χ_M^{-1} vs. T plots for **1**.

As already described, compound **1** has a pillared layered structure in which the inorganic layers are separated by the organic groups of pna^{3-}. Within the inorganic layer, chains made up of $Cu_2(\mu_3\text{-}O)_2$ dimers and CuO_6 octahedra through O1W and carboxylate linkages are found, which are interconnected by the phosphonate bridges. There are at least four exchange pathways in propagating the magnetic interactions within the inorganic layer in **1**, for example, through the μ_3-O(P), μ_2-OH_2, O–C–O, and O–P–O bridges. Considering that the Cu(1)–O(1W)–Cu(2) bond angle is 119.4(1)° and the O(1W) atom occupies the axial positions with long Cu–O(1W) bond lengths [2.426(3)–2.560(3) Å], very weak antiferromagnetic interaction would be expected through the O(1W) bridge. Very weak antiferromagnetic exchange coupling could also mediate through μ_3-O(P) in **1**, because the Cu–O–Cu angle [99.89(13)°] is much larger than those anticipated for a ferromagnetic interaction in planar hydroxy-bridged copper(II) dimers (< 97.5°)[20] and alkoxido-bridged copper(II) complexes (< 95.8°).[21] Noting that the O–P–O pathway is less efficient than the O–C–O pathway due to electron localization, the dominant ferromagnetic interaction in **1** is mainly attributed to the exchange couplings through the O–C–O pathway. It has been found that weak ferromagnetic interactions can be propagated in the carboxylate-bridged copper(II) compounds in which the carboxylate adopts the *anti-syn* conformation and the Cu–O–C–O–Cu skeleton deviates from planarity,[22]

which is also observed in compound **1**. Therefore, the susceptibility data were analyzed by using a Cu_3 trimer model based on the Hamiltonian:

$$\hat{H} = -2J \sum_{j>i=1}^{3} \hat{S}_i \cdot \hat{S}_j$$

$$\chi_{trimer} = \frac{Ng^2\beta^2}{4kT} \cdot \frac{1+\exp(2J/kT)+10\exp(3J/kT)}{1+\exp(2J/kT)+2\exp(3J/kT)}$$

$$\chi_M = \frac{\chi_{trimer}}{1-(zj'/Ng^2\beta^2)\chi_{trimer}}$$

where zj' accounts for the inter-trimer interactions. A best fit is obtained in the temperature range 9–300 K with parameters g = 2.19, J = 4.79 cm^{-1} and zj' = –0.70 cm^{-1} (Figure 6, solid line). The decline of $\chi_M T$ below 9.0 K can be caused by the inter-trimer antiferromagnetic exchange and the zero-field splitting of the ground state.

In order to determine whether a long-range ordering occurs at low temperature, the temperature-dependent zero-field ac susceptibility is measured under H_{ac} = 1 Oe and a frequency of 10 Hz. Figure 7 clearly shows a maximum of the in-phase signal [$\chi_m'(T)$] appearing at 4.1 K and the absence of the out-of-phase signal [$\chi_m''(T)$], indicating that compound **1** has an antiferromagnetic (AF) ground state. The field dependence of magnetization is also measured at 1.8 K. As shown in Figure 8, the magnetization increases linearly with increasing field in the range 0–7.0 kOe, followed by a slight upturn in the field range 7.0–20 kOe, and reaches 0.90 $N\beta$ at 20 kOe. Above 20 kOe, a linear field-dependent magnetization is again observed until a second upturn occurs at approximately 60 kOe. The slightly S-shaped curve could arise from a stepped spin flop transition (Figure 8). The critical fields, determined by the d($M/N\beta$)/dH vs. H plot, are approximately 12.0 and 50 kOe. The magnetization at 70 kOe (2.75 $N\beta$) does not reach a saturation value of 3.3 $N\beta$ for three independent S = 1/2 spins with g = 2.2.

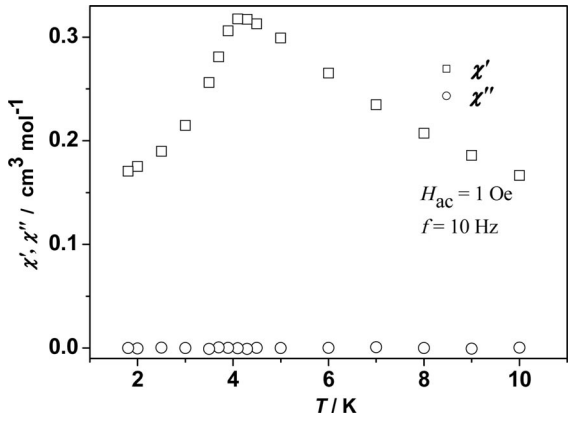

Figure 7. Temperature dependence of zero-field ac magnetic susceptibility for **1**.

It could be of interest to compare the magnetic behavior of **1** with that of $Cu_3(pin)_2(H_2O)_2$.[19] Although the two compounds possess similar pillared layered structures, compound **1** shows an AF ground state with a spin flop behavior, while compound $Cu_3(pin)_2(H_2O)_2$ displays a ferromagnetic ground state with the occurrence of long-range ordering below 2.2 K. Such remarkable difference between the magnetic properties of the two compounds could be related to the difference in their interlayer distances in addition to other structural differences. A shorter interlayer distance in **1** (8.771 Å) favors an AF interaction, while a longer interlayer distance in $Cu_3(pin)_2(H_2O)_2$ (9.021 Å) favors a ferromagnetic interaction between the neighboring layers. A similar phenomenon has been observed in other organic–inorganic hybrid materials with layered or pillared layered structures.[23]

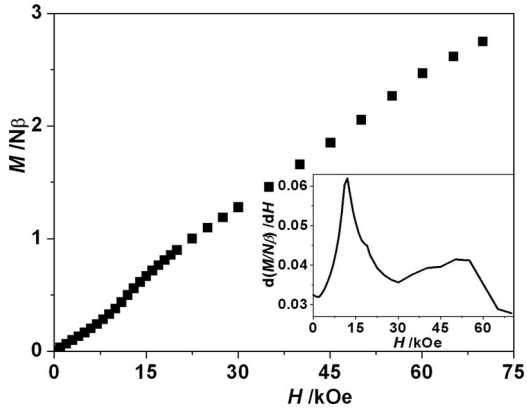

Figure 8. Magnetization of **1** at 1.8 K. Inset: d($M/N\beta$)/dH vs. H curve.

Magnetic Properties of 2

The temperature-dependent molar magnetic susceptibilities of **2** were measured at 2 kOe in the temperature range 1.8–300 K. The room temperature $\chi_M T$ value of 9.63 $cm^3\,K\,mol^{-1}$ per Co_3 unit is much higher than the expected spin-only value of 5.63 $cm^3\,K\,mol^{-1}$ for S = 3/2, attributed to the orbital contribution arising from the high-spin octahedral Co^{II} centers.[24] Upon cooling, the $\chi_M T$ decreases slowly and reaches a minimum of 7.27 $cm^3\,K\,mol^{-1}$ at 22 K. Then it increases suddenly to a maximum of 14.85 $cm^3\,K\,mol^{-1}$ at 6 K, suggesting a ferrimagnetic-like character (Figure 9).

Compound **2** has a pillared layered structure similar to that of **1**. In this case, the Co2–O–Co2 angle over the μ_3-O1(P) bridge [97.93(1)°] is smaller than that in **1**. The carboxylate group also adopts the *anti-syn* conformation, the Co–O–C–O–Co skeleton deviating from planarity. Hence, weak ferromagnetic exchange coupling could be anticipated through the μ_3-O1(P) and carboxylate pathways.[25] Nevertheless, the Co1–O1W–Co2 angle [126.0(1)°] is much larger than that in **1** [119.4(1)°] and the Co–O1W distances are much shorter, which could lead to a dominant antiferromagnetic interaction through the μ_2-O1W bridge. Although the dominant exchange coupling between the magnetic centers is antiferromagnetic, the odd number of the Co^{II} ions within the asymmetric unit results in a nonzero net mag-

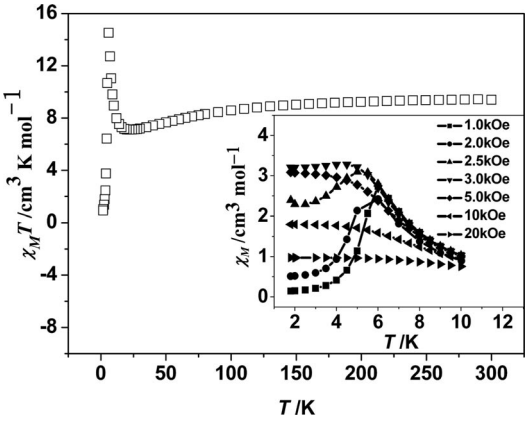

Figure 9. $\chi_M T$ vs. T for **2**. Inset: χ_M vs. T plots at different external fields.

netic moment corresponding to an intralayer ferrimagnetism, which has been observed in a few other homometallic systems.[13–15,26] The decline of $\chi_M T$ below 6 K can be caused by the interlayer antiferromagnetic exchange and/or the zero-field splitting of the anisotropic high-spin Co^{II} ion.

The inset of Figure 9 shows the χ_M vs. T plots of **2** measured at different external fields. Clearly, a sharp peak is observed at approximately 6.0 K at a low field of 1.0 kOe, suggesting an AF ground state. The AF ground state is confirmed by the temperature-dependent zero-field ac magnetic susceptibility $\chi_M'(T)$, which shows a peak at approximately 6.2 K at H_{ac} = 1 Oe and a frequency of 10 Hz as well as the absence of an out-of-phase component (χ_M'') at this temperature (Figure 10). The AF ground state observed in **2** can arise from antiparallel alignment of the ferrimagnetic layers. The disappearance of the peak in the χ_M vs. T plots above 3.0 kOe indicates that a field-induced magnetic transition may occur. The field-dependent magnetization of **2** at 1.8 K reveals an S-shaped curve, typical for metamagnetic transition from an antiferromagnetic state to a ferrimagnetic state (Figure 11). The critical field, determined by the d(M/$N\beta$)/dH vs. H curve, is approximately 3 kOe (Figure 11, inset). The magnetization value at 9 kOe is 3.0 $N\beta$ per formula, close to that expected for one uncompensated Co^{II} ion. No saturation is achieved when the external field increases to 70 kOe.

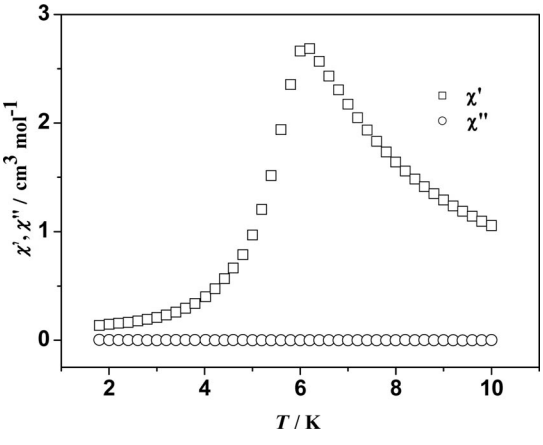

Figure 10. Temperature dependence of zero-field ac magnetic susceptibility for **2**.

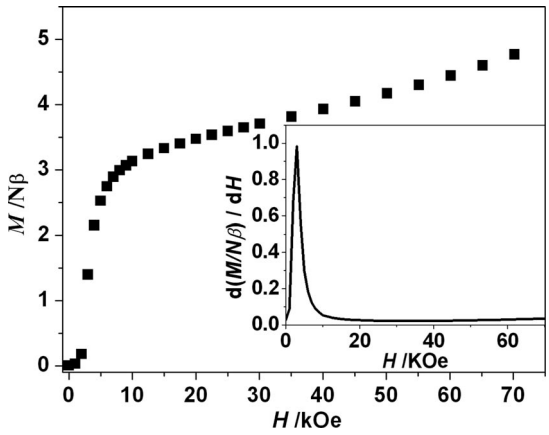

Figure 11. Magnetization of **2** at 1.8 K. Inset: d(M/$N\beta$)/dH vs. H curve.

Conclusions

We report two isostructural metal phosphonates with formula $Cu_3(pna)_2(H_2O)_2$ (**1**) and $Co_3(pna)_2(H_2O)_2$ (**2**), showing pillared layered structures. Both have an antiferromagnetic ground state but exhibit different field-induced magnetic behavior: a spin flop transition is observed in **1**, whereas **2** shows metamagnetic behavior. Further work is in progress to explore new layered or pillared layered metal phosphonates with interesting magnetic properties.

Experimental Section

Materials and Measurements: The chemical reagents are commercially available and were used without further purification. The 6-phosphononicotinic acid ($pnaH_3$) was synthesized according to the literature.[27] Elemental analysis was performed with a PE 240C elemental analyzer. The infrared spectra were recorded with a VECTOR 22 spectrometer by using KBr pellets. Thermogravimetric analyses were performed with a Perkin-Elmer Pyris 1 TGA instrument in the range 30–800 °C under a nitrogen flow at a heating rate of 10 °C min^{-1}. Powder X-ray diffraction (XRD) data were collected with a Shimadzu XRD-6000 X-ray diffractometer with Cu-K_α radiation (λ = 1.54056 Å). The magnetic susceptibility data were obtained on polycrystalline samples by using a Quantum Design MPMS-XL7 SQUID magnetometer. The data were corrected for diamagnetic contributions of both the sample holder and the compound obtained from Pascal's constant.[24]

$Cu_3(pna)_2(H_2O)_2$ (1): A mixture of $CuCl_2{\cdot}2H_2O$ (0.1 mmol, 0.0172 g), $pnaH_3$ (0.1 mmol, 0.0203 g), and H_2O (8 mL) was placed in a Teflon-lined stainless steel vessel. The mixture was sealed and heated at 140 °C for 3 d, then the reaction system was cooled to room temperature. Light blue block-like crystals of **1** were obtained in a yield of 30% (based on Cu). $C_{12}H_{10}Cu_3N_2O_{12}P_2$ (626.80): calcd. C 23.01, H 1.66, N 4.46; found C 23.00, H 1.70, N 4.44. IR (KBr): $\tilde{\nu}$ = 3409 (s), 1600 (s), 1552 (m), 1400 (s), 1147 (s), 1083 (s), 970 (s), 858 (w), 781 (m), 744 (s), 595 (s), 522 (m) cm^{-1}. Thermal

analysis shows a weight loss of 5.9% in the temperature range 25–450 °C, close to the calculated value for the release of two coordination water molecules (5.7%).

$Co_3(pna)_2(H_2O)_2$ (2): A mixture of $Co(ClO_4)_2·6H_2O$ (0.1 mmol, 0.0366 g), $pnaH_3$ (0.1 mmol, 0.0203 g), piperazine (0.2 mmol, 0.0172 g) and H_2O (8 mL), with the pH adjusted to 3.5 by dilute $HClO_4$ solution (1.0 mol/L), was placed in a Teflon-lined stainless steel vessel. The mixture was sealed and heated at 180 °C for 3 d, and then the reaction system was cooled to room temperature. Purple crystals were obtained in a yield of 25% (based on Co). $C_{12}H_{10}Co_3N_2O_{12}P_2$ (612.96): calcd. C 23.51, H 1.64, N 4.57; found C 23.53, H 1.71, N 4.52. IR (KBr): $\tilde{\nu}$ = 3424 (s), 1602 (s), 1546 (m), 1409 (s), 1147 (s), 1081 (s), 987 (s), 858 (w), 784 (m), 740 (s), 609 (s), 524 (m) cm^{-1}. Thermal analysis shows a weight loss of 6.1% in the temperature range 25–450 °C, close to the calculated value for the release of two coordination water molecules (5.9%).

Crystallographic Studies: Single crystals with dimensions $0.25 \times 0.20 \times 0.18$ mm^3 for **1** and $0.20 \times 0.16 \times 0.12$ mm^3 for **2** were selected for indexing and intensity data collection with a Bruker SMART APEX CCD diffractometer equipped with graphite monochromated Mo-K_α (λ = 0.71073 Å) radiation at 293 K. The data were collected in the θ range 2.32 to 25.49° for **1** and 2.33 to 25.50° for **2** by using a narrow-frame method with scan widths of 0.308° in ω and an exposure time of 5 s per frame. The numbers of the observed and unique reflections are 2180 and 1518 (R_{int} = 0.0327) for **1** and 2169 and 1527 (R_{int} = 0.0184) for **2**, respectively. The data were integrated by using the Siemens *SAINT* program;[28] the intensities were corrected for the Lorentz factor, polarization, air absorption, and absorption due to variation in the path length through the detector faceplate. Absorption corrections were applied. The structures were solved by direct methods and refined on F^2 by full-matrix least-squares with *SHELXTL*.[29] All non-hydrogen atoms were refined anisotropically. All hydrogen atoms except those attached to water molecules were put in calculated positions. The hydrogen atoms of water molecules were found from the Fourier maps. All hydrogen atoms were refined isotropically with the isotropic vibration parameters related to the non-hydrogen atoms to which they were bonded. Crystallographic and refinement details of **1** and **2** are listed in Table 3.

Table 3. Crystallographic data for compounds **1** and **2**.

Compound	**1**	**2**
Formula	$C_{12}H_{10}Cu_3N_2O_{12}P_2$	$C_{12}H_{10}Co_3N_2O_{12}P_2$
M	626.78	612.95
Crystal system	triclinic	triclinic
Space group	$P\bar{1}$	$P\bar{1}$
a /Å	5.9778(12)	6.0717(18)
b /Å	8.3606(18)	8.089(2)
c /Å	9.1921(19)	9.112(3)
α /°	83.697(4)	88.314(5)
β /°	72.625(4)	73.692(5)
γ /°	72.405(4)	77.059(5)
V /Å^3	417.83(15)	418.4(2)
Z	1	1
D_c /g cm^{-3}	2.499	2.433
μ /mm^{-1}	4.053	3.209
F(000)	309	303
GooF on F^2	1.062	1.017
$R1$, $wR2$[a] [$I>2\sigma(I)$]	0.0363, 0.0736	0.0385, 0.01023
$R1$, $wR2$[a] (all data)	0.0443, 0.0759	0.0446, 0.01068
$(\Delta\rho)_{max}$, $(\Delta\rho)_{min}$ /e Å^{-3}	0.516, –0.506	0.847, –0.513

[a] $R1 = \Sigma||F_o| - |F_c||/\Sigma|F_o|$; $wR2 = [\Sigma w(F_o^2 - F_c^2)^2/\Sigma w(F_o^2)^2]^{1/2}$.

CCDC-746215 and -746216 contain the supplementary crystallographic data for this paper. These data can be obtained free of charge from The Cambridge Crystallographic Data Centre via www.ccdc.cam.ac.uk/data_request/cif.

Supporting Information (see footnote on the first page of this article): TGA curves and XRD patterns for compounds **1** and **2**, the inorganic layer structure of **2**, and ZFC/FC curves for **2** are provided.

Acknowledgments

This work is supported by the Natural Science Funds (NSF) of China (No. 20631030), the National Basic Research Program of China (2007CB925102, 2010CB923402), the NSF of Jiangsu Province (No. BK2009009) and the NSF of China for Creative Research Group (No. 20721002). We thank Prof. You Song and Dr. Tian-Wei Wang for magnetic measurements and valuable discussions.

[1] a) A. Clearfield, *Prog. Inorg. Chem.* **1998**, *47*, 371–510; b) S. R. Miller, G. M. Pearce, P. A. Wright, F. Bonino, S. Chavan, S. Bordiga, I. Margiolaki, N. Guillou, G. Férey, S. Bourrelly, P. L. Llewellyn, *J. Am. Chem. Soc.* **2008**, *130*, 15967–15981; c) E. Brunet, H. M. H. Alhendawi, C. Cerro, M. J. Mata, O. Juanes, J. C. Rodríguez-Ubis, *Angew. Chem. Int. Ed.* **2006**, *45*, 6918–6920.

[2] a) L.-Q. Ma, C. Abney, W.-B. Lin, *Chem. Soc. Rev.* **2009**, *38*, 1248–1256; b) S. Chessa, N. J. Clayden, M. Bochmann, J. A. Wright, *Chem. Commun.* **2009**, 797–799; c) W. J. Youngblood, S. H. A. Lee, Y. Kobayashi, E. A. Hernandez-Pagan, P. G. Hoertz, T. A. Moore, A. L. Moore, D. Gust, T. E. Mallouk, *J. Am. Chem. Soc.* **2009**, *131*, 926–927; d) S.-S. Bao, L.-F. Ma, Y. Wang, L. Fang, C.-J. Zhu, Y.-Z. Li, L.-M. Zheng, *Chem. Eur. J.* **2007**, *13*, 2333.

[3] a) J.-G. Mao, *Coord. Chem. Rev.* **2007**, *251*, 1493 and references cited therein; b) X.-G. Liu, K. Zhou, J. Dong, C.-J. Zhu, S.-S. Bao, L.-M. Zheng, *Inorg. Chem.* **2009**, *48*, 1901–1905; c) E. Brunet, H. M. H. Alhendawi, O. Juanes, L. Jiménez, J. C. Rodríguez-Ubis, *J. Mater. Chem.* **2009**, *19*, 2494–2502.

[4] For example: a) S. Maheswaran, G. Chastanet, S. J. Teat, T. Mallah, R. Sessoli, W. Wernsdorfer, R. E. P. Winpenny, *Angew. Chem. Int. Ed.* **2005**, *44*, 5044–5048; b) J.-T. Li, T. D. Keene, D.-K. Cao, S. Decurtins, L.-M. Zheng, *CrystEngComm* **2009**, *11*, 1255–1260; c) B.-B. Yang, A. V. Prosvirin, Y.-Q. Guo, J.-G. Mao, *Inorg. Chem.* **2008**, *47*, 1453–1459; d) S. Konar, A. Clearfield, *Inorg. Chem.* **2008**, *47*, 3489–3491; e) E. M. Bauer, C. Bellito, G. Righini, M. Colapietro, G. Portalone, M. Drillon, P. Rabu, *Inorg. Chem.* **2008**, *47*, 10945–10952.

[5] a) J. Monot, M. Petit, S. M. Lane, I. Guisle, J. Léger, C. Tellier, D. R. Talham, B. Bujoli, *J. Am. Chem. Soc.* **2008**, *130*, 6243–6251; b) J. Amalric, P. H. Mutin, G. Guerrero, A. Ponche, A. Sotto, J. P. Lavigne, *J. Mater. Chem.* **2009**, *19*, 141–149; c) N. Adden, L. J. Gamble, D. G. Castner, A. Hoffmann, G. Gross, H. Menzel, *Langmuir* **2006**, *22*, 8197–8204.

[6] G. K. H. Shimizu, R. Vaidhyanathan, J. M. Taylor, *Chem. Soc. Rev.* **2009**, *38*, 1430–1449.

[7] a) R. L. Carlin, A. J. Van-Duyneveldt, *Magnetic Properties of Transition Metal Compounds*, Springer-Verlag, New York, **1977**; b) R. L. Carling, *Magnetochemistry*, Springer-Verlag, Berlin, **1986**; c) C. Bellitto in *Magnetism: Molecules to Materials* (Eds.: J. S. Miller, M. Drillon), Wiley-VCH, Weinheim, **2001**, vol. 2, pp. 425–456; d) P. Rabu, M. Drillon, *Adv. Engineer. Mater.* **2003**, *5*, 189–210 and references cited therein; e) M. Kurmoo, *Chem. Soc. Rev.* **2009**, *38*, 1353–1379.

[8] a) X.-Y. Wang, Z.-M. Wang, S. Gao, *Inorg. Chem.* **2008**, *47*, 5720–5726; b) J. H. Yoon, D. W. Ryu, H. C. Kim, S. W. Yoon, B. J. Suh, C. S. Hong, *Chem. Eur. J.* **2009**, *15*, 3661–3665; c) H. Arora, F. Lloret, R. Mukherjee, *Inorg. Chem.* **2009**, *48*, 1158–

1167; d) Z. Duan, Y. Zhang, B. Zhang, D.-B. Zhu, *Inorg. Chem.* **2008**, *47*, 9152–9154; e) M. Clemente-León, E. Coronado, M. C. Giménez-López, A. Soriano-Portillo, J. C. Waerenborgh, F. S. Delgado, C. Ruiz-Pérez, *Inorg. Chem.* **2008**, *47*, 9111–9120; f) A. V. Palii, O. S. Reu, S. M. Ostrovsky, S. I. Klokishner, B. S. Tsukerblat, Z.-M. Sun, J.-G. Mao, A. V. Prosvirin, H.-H. Zhao, K. R. Dunbar, *J. Am. Chem. Soc.* **2008**, *130*, 14729–14738.

[9] a) S. Chattopadhyay, M. G. B. Drew, C. Diaz, A. Ghosh, *Dalton Trans.* **2007**, 2492–2494; b) H. P. Jia, W. Li, Z. F. Ju, J. Zhang, *Chem. Commun.* **2008**, 371–373; c) M.-H. Zeng, W.-X. Zhang, X.-Z. Sun, X.-M. Chen, *Angew. Chem. Int. Ed.* **2005**, *44*, 3079–3082; d) C. Aoki, T. Ishida, T. Nogami, *Inorg. Chem.* **2003**, *42*, 7616–7625; e) M. Monfort, I. Resino, J. Ribas, H. Stoeckli-Evans, *Angew. Chem. Int. Ed.* **2000**, *39*,191–193.

[10] a) G. Lazari, T. C. Stamatatos, C. P. Raptopoulou, V. Psycharis, M. Pissas, S. P. Perlepes, A. K. Boudalis, *Dalton Trans.* **2009**, 3215–3221; b) Y.-B. Lu, M.-S. Wang, W.-W. Zhou, G. Xu, G.-C. Guo, J.-S. Huang, *Inorg. Chem.* **2008**, *47*, 8935–8942; c) Y. S. You, J. H. Yoon, H. C. Kim, C. S. Hong, *Chem. Commun.* **2005**, 4116–4118.

[11] a) C. L. M. Pereira, E. F. Pedroso, H. O. Stumpf, M. A. Novak, L. Ricard, R. Ruiz-García, E. Riviète, Y. Journaux, *Angew. Chem. Int. Ed.* **2004**, *43*, 955–958; b) E. Q. Gao, Y. F. Yue, S. Q. Bai, Z. He, C. H. Yan, *J. Am. Chem. Soc.* **2004**, *126*, 1419–1429; c) Y. Z. Zhang, S. Gao, H. L. Sun, G. Su, Z. M. Wang, S. W. Zhang, *Chem. Commun.* **2004**, 1906–1907; d) Y.-Q. Tian, C.-X. Cai, X.-M. Ren, C.-Y. Duan, Y. Xu, S. Gao, X.-Z. You, *Chem. Eur. J.* **2003**, *9*, 5673–5685.

[12] L.-M. Zheng, S. Gao, H.-H. Song, S. Decurtins, A. J. Jacobson, X.-Q. Xin, *Chem. Mater.* **2002**, *14*, 3143–3147.

[13] P. Yin, L.-M. Zheng, S. Gao, X.-Q. Xin, *Chem. Commun.* **2001**, 2346–2347.

[14] P. Yin, S. Gao, L.-M. Zheng, Z.-M. Wang, X.-Q. Xin, *Chem. Commun.* **2003**, 1076–1077.

[15] S.-Z. Hou, D.-K. Cao, X.-G. Liu, Y.-Z. Li, L.-M. Zheng, *Dalton Trans.* **2009**, 2746–2750.

[16] T.-H. Yang, Y. Liao, L.-M. Zheng, R. E. Dinnebier, Y.-H. Su, J. Ma, *Chem. Commun.* **2009**, 3023–3025.

[17] P. Rabu, P. Janvier, B. Bujoli, *J. Mater. Chem.* **1999**, *9*, 1323–1326.

[18] D. Y. Kong, A. Clearfield, *Cryst. Growth Des.* **2005**, *5*, 1263–1270.

[19] Y.-F. Yang, Y.-S. Ma, L.-R. Guo, L.-M. Zheng, *Cryst. Growth Des.* **2008**, *8*, 1213–1217.

[20] W. H. Crawford, H. W. Richardson, J. R. Wasson, D. J. Hodgson, W. E. Hatfield, *Inorg. Chem.* **1976**, *15*, 2107.

[21] L. Merz, W. Haase, *J. Chem. Soc., Dalton Trans.* **1980**, 875.

[22] a) C. Ruiz-Pérez, J. Sanchiz, M. H. Molina, F. Lloret, M. Julve, *Inorg. Chem.* **2000**, *39*, 1363–1370; b) J. Pasán, J. Sanchiz, C. Ruiz-Pérez, J. Campo, F. Lloretd, M. Julve, *Chem. Commun.* **2006**, 2857–2859; c) J. Pasán, J. Sanchiz, C. Ruiz-Pérez, F. Lloret, M. Julve, *Inorg. Chem.* **2005**, *44*, 7794–7801.

[23] a) V. Laget, C. Hornick, P. Rabu, M. Drillon, R. Ziessel, *Coord. Chem. Rev.* **1998**, *178–180*, 1533; b) Z.-C. Zhang, L.-M. Zheng, *Inorg. Chem. Commun.* **2008**, *11*, 1243–1245; c) D.-K. Cao, X.-J. Xie, Y.-Z. Li, L.-M. Zheng, *Dalton Trans.* **2008**, 5008–5015.

[24] O. Kahn, *Molecular Magnetism*, VCH Publishers, Inc., New York, **1993**.

[25] O. Fabelo, J. Pasán, L. Cañadillas-Delgado, F. S. Delgado, F. Lloret, M. Julve, C. Ruiz-Pérez, *Inorg. Chem.* **2009**, *48*, 6086–6095.

[26] a) S. Konar, P. S. Mukherjee, E. Zangrando, F. Floret, N. R. Chaudhuri, *Angew. Chem. Int. Ed.* **2002**, *41*, 1561–1563; b) M.-H. Zeng, M.-C. Wu, H. Liang, Y.-L. Zhou, X.-M. Chen, S.-W. Ng, *Inorg. Chem.* **2007**, *46*, 7241–7243; c) R. Patel, M. T. Weller, D. J. Price, *Dalton Trans.* **2007**, 4034–4039.

[27] J. S. Loran, R. A. Naylor, A. Williams, *J. Chem. Soc. Perkin Trans. 2* **1976**, 1444.

[28] *SAINT*, *Program for Data Extraction and Reduction*, Siemens Analytical X-ray Instruments, Madison, WI, 1994–**1996**.

[29] *SHELXTL* (version 5.0), Reference Manual, Siemens Industrial Automation, Analytical Instruments, Madison, WI, **1995**.

Received: September 3, 2009
Published Online: January 12, 2010

